Amorphous phase-segregated copoly(ether)esterurethane thermoset networks with oligo(propylene glycol) and oligo [(*rac*-lactide)-*co*-glycolide] segments: synthesis and characterization

Jörg Zotzmann · Armin Alteheld · Marc Behl · Andreas Lendlein

Abstract Completely amorphous copoly(ether)ester networks based on oligo(propylene glycol) and oligo[(*rac*-dilactide)-*co*-glycolide] segments were synthesized by crosslinking star-shaped hydroxyl-telechelic cooligomers using an aliphatic low-molecular weight diisocyanate. Two different network architectures were applied exhibiting differences in the phase-separation behavior. For networks from oligo(propylene glycol)-*block*-oligo[(*rac*-lactide)-*co*-glycolide] triols (G^{3}OPG-*bl*-OLG) only one glass transition was obtained. However, networks from a mixture of oligo(propylene glycol) triols (G^{3}OPG) and oligo[(*rac*-lactide)-*co*-glycolide] tetrols (P^{4}OLG) with a ratio of components in a certain range show two glass transition temperatures (T_g) being attributed to two segregated amorphous phases. In this way a wide spectrum of mechanical properties can be realized and adjusted to the requirements of a specific application.
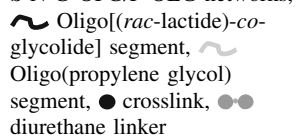
1 Introduction

A challenge of biomaterial development is the combination of material properties and functions such as elastic properties and degradability to the requirements of specific applications. Amorphous copolymers of lactic acid and glycolic acid have been explored extensively as degradable biomaterials [1, 2]. Unlike semi-crystalline polymers they show a more homogeneous degradation being advantageous for application in implants. The rate of their hydrolytic degradation can be varied by the comonomer ratio [3–6]. With a glass transition temperature (T_g) between 40 and 55°C these materials are glassy at room temperature as well as at body temperature and posses a high E-modulus. The elastic properties below body temperature can be controlled by incorporating a second amorphous phase having a low T_g [7, 8]. However, highly elastic copolymers with a low E-modulus tend to yield. Covalent crosslinking of polyesters forming polymer networks provides form stability while the elasticity is maintained [9].

An example are AB polymer networks obtained by photo polymerization of dimethacrylated poly[(L-lactide)-*ran*-glycolide)] chain segments, whose elastic properties below body temperature were improved by incorporating a second amorphous phase such as polymers from low-molecular weight acrylates [10]. In another approach, the elasticity determining phase was integrated into the polymer chains being realized in multiphase photosets prepared from amorphous ABA triblock macrodimethacrylates based on poly(*rac*-lactide)-*block*-poly(propylene oxide)-*block*-poly(*rac*-lactide). Atactic poly(propylene glycol) was selected as elastic component since it is amorphous, immiscible with the first component, and shows a low T_g [11, 12]. Variation of the *rac*-lactide content of the triblock polymers showed that a minimum block length was required to obtain two distinct T_gs as a result of phase separation, which influences in this way the thermal properties [11]. Another drawback of such polymer networks based on macrodimethacrylates is the irregular distribution of netpoints within the polymer network structure.

J. Zotzmann · M. Behl · A. Lendlein (✉)
Centre of Biomaterial Development, Institute of Polymer Research, GKSS Research Center, Kantstr. 55, 14513 Teltow, Germany
e-mail: lendlein@gkss.de; andreas.lendlein@gkss.de

A. Alteheld
BASF Aktiengesellschaft, GKT/F-B001, 67056 Ludwigshafen, Germany

Fig. 1 Comparison of the two applied network architectures; **a** N-G^{3}OPG-*bl*-OLG networks, **b** N-G^{3}OPG/P^{4}OLG networks, ∿ Oligo[(*rac*-lactide)-*co*-glycolide] segment, ∿ Oligo(propylene glycol) segment, ● crosslink, ●● diurethane linker
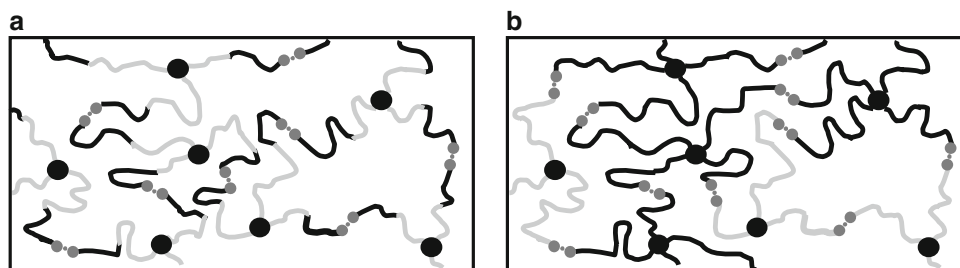
Therefore, the adjustability of the thermal and mechanical properties of these networks is limited due to the required molecular weight and the confined control over the degree of crosslinking.

Biodegradable amorphous copolyesterurethane networks with a defined polymer network structure were prepared from star-shaped poly[*rac*(lactide)-*co*-glycolide] segments, which were crosslinked by reaction of their terminal functional groups with a low-molecular weight diisocyanate [13]. Adjustability of mechanical properties was enabled by the control of molecular parameters such as functionality of crosslinks and the length of chain segments [14–20].

We report on the investigation whether such copolyesterurethane networks with defined netpoint functionality can be synthesized and how the introduction of a second amorphous phase influences the mechanical properties. Poly(propylene glycol) was chosen as a second amorphous phase. Microscopic phase segregation within the amorphous networks was expected to lead to two distinct glass transitions. Two concepts of network architecture were investigated, which can be distinguished by the star-shaped precursors that were crosslinked with diisocyanate:

(1) In the first concept one type of star-shaped precursor, already containing the two different oligomer segments within its linear chains was crosslinked (see Fig. 1a).

(2) In the second concept a mixture of two different star-shaped precursors containing the two different chain segments respectively were reacted to form the polymer network (see Fig. 1b).

2 Materials and methods

2.1 Materials

rac-Dilactide (**3**, mixture from D,D-dilactide and L,L-dilactide, no *meso*-dilactide was detectable in ^{1}H-NMR spectra, Sigma-Aldrich) and diglycolide (**4**, Boehringer Ingelheim) were applied after recrystallization from ethyl acetate. TMDI (Sigma-Aldrich) was distilled in vacuum prior to reaction. Pentaerythrite (**2**, Sigma-Aldrich), dibutyltin oxide (DBTO, Fluka), and dibutyltin dilaurate (DBTDL,

Merck) were used as received. Oligo(propylene glycol)s (**1**, Sigma-Aldrich) with a number average molecular weight (M_n) of 1000, 3000 and 6000 g mol^{-1} were dried by stirring at 70°C in high vacuum for about 3 h.

2.2 Polymer synthesis

Synthesis of the oligo(propylene glycol)-*block*-oligo[(*rac*-lactide)-*co*-glycolide] triols (G^{3}OPG-bl-OLG): The polymerization was carried out by solvent free ring opening polymerization (ROP) under nitrogen atmosphere at 150°C. The reaction mixture from *rac*-dilactide **3**, diglycolide **2** and the oligo(propylene glycol) triol **1** was heated, stirred for 5 days and then cooled to room temperature. The cooligomers were dissolved in a 6–10-fold excess of CH$_2$Cl$_2$ and subsequently precipitated in hexane. The precipitate was washed with hexane fraction and dried to constant weight at 80°C in a vacuum oven. Quantities of the reactants are given in Table 1.

Synthesis of the oligo[(*rac*-lactide)-*co*-glycolide] tetrol (**6**): The polymerization was carried out in bulk under a nitrogen atmosphere at 130°C as described previously [13]. A P^{4}OLG tetrol with a glycolide content of 17 wt% and a M_n of 10000 g mol^{-1} was synthesized.

Formation of the polymer networks from G^{3}OPG-*bl*-OLG segments: The hydroxyl-telechelic cooligomers were dissolved in a tenfold excess of CH$_2$Cl$_2$ under nitrogen atmosphere. A defined amount of TMDI was added to the solution under stirring. A molar ratio of isocyanate to hydroxyl functional groups of 1.05 to 1 (based on M_n values from ^{1}H-NMR spectroscopy) was adjusted in order to compensate the loss of active isocyanate groups due to traces of water. After 5 min, the reaction mixture was poured into PTFE dishes and kept under a constant nitrogen flow for 24 h at room temperature to evaporate the solvent during polymer network formation. In order to complete film crosslinking, the films were kept at 80°C under reduced pressure (100 mbar) for another 4 days. The crude films were extracted with chloroform and dried to constant weight in vacuum (0.1 mbar) at 80°C. The quantities are summarized in Table 2.

Formation of the polymer networks from G^{3}OPG and P^{4}OLG segments (Fig. 1b): The polyaddition reaction was

Table 1 Synthesis of G^{3}OPG-*bl*-OLG triols

Sample ID[a]	*rac*-Dilactide		Diglycolide		G^{3}OPG triol		μ_{OPG} (wt%)[b]
	n (mmol)	*m* (g)	*n* (mmol)	*m* (g)	*n* (mmol)[c]	*m* (g)	
G^{3}OPG(1)-*bl*-OLG(2)	44.3	6.38	9.74	1.13	8.06	7.50	50.0
G^{3}OPG(1)-*bl*-OLG(4)	66.3	9.56	14.60	1.69	4.03	3.75	25.0
G^{3}OPG(1)-*bl*-OLG(6)	73.8	10.63	16.20	1.88	2.69	2.50	16.7
G^{3}OPG(1)-*bl*-OLG(9)	78.6	11.33	17.20	2.00	1.80	1.67	11.1
G^{3}OPG(3)-*bl*-OLG(4)	22.1	3.19	4.82	0.56	3.24	11.25	75.0
G^{3}OPG(3)-*bl*-OLG(6)	44.3	6.38	9.74	1.13	2.16	7.50	50.0
G^{3}OPG(3)-*bl*-OLG(9)	59.0	8.50	12.90	1.50	1.44	5.00	33.3
G^{3}OPG(3)-*bl*-OLG(9)	29.5	4.25	6.46	0.75	1.79	10.00	67.7
G^{3}OPG(6)-*bl*-OLG(12)	44.3	6.38	9.74	1.13	1.34	7.50	50.0

[a] G^{3}OPG(x)-*bl*-OLG(y) are star-shaped precursors (G^3, three armed glycerol based star) with oligo(propylene glycol) (OPG) chains, the M_n ($x \times 1000$ g mol^{-1}) given in *parentheses*, where blocks (*bl*) of oligo(lactide-*co*-glycolide) (OLG), whose M_n ($y \times 1000$ g mol^{-1}) is given in *parentheses*, are polymerized to

[b] Expected content of OLG for the product as calculated from the starting materials

[c] Calculation based on the M_n-values obtained from ^{1}H-NMR spectroscopic data

Table 2 Synthesis of N-G^{3}OPG-*bl*-OLG networks

Sample ID[a]	G^{3}OPG-*bl*-OLG		TMDI	
	n (mmol)[b]	*m* (g)	*n* (mmol)	*V* (µl)
N-G^{3}OPG(1)-*bl*-OLG(2)	0.45	1.02	0.71	147.2
N-G^{3}OPG(1)-*bl*-OLG(4)	0.25	1.05	0.39	81.6
N-G^{3}OPG(1)-*bl*-OLG(6)	0.16	1.07	0.26	53.8
N-G^{3}OPG(1)-*bl*-OLG(9)	0.11	0.98	0.17	35.4
N-G^{3}OPG(3)-*bl*-OLG(4)	0.23	0.98	0.36	75.7
N-G^{3}OPG(3)-*bl*-OLG(6)	0.21	1.37	0.33	69.2
N-G^{3}OPG(3)-*bl*-OLG(9)	0.12	1.06	0.18	38.3

[a] N-G^{3}OPG(x)-*bl*-OLG(y) are polymer networks (N) obtained by crosslinking G^{3}OPG(x)-*bl*-OLG(y) precursors, for G^{3}OPG(x)-*bl*-OLG(y) see Table 1 note a

[b] Calculation based on the M_n-values obtained from ^{1}H-NMR spectroscopic data

carried out as described for the polymer networks from G^{3}OPG-*bl*-OLG. After addition of diisocyanate to the reaction mixture DBTDL (100 µl/g starting material) was added as catalyst so that the reaction started at room temperature. The quantities of the reactants are shown in Table 3.

2.3 Polymer characterization methods

^{1}H-NMR spectra (400 MHz) were recorded on a VARIAN INOVA 400 in deuterated chloroform (CDCl$_3$) or dimethylsulfoxide (DMSO-d$_6$) with tetramethylsilane as internal standard. The comonomer content and the number average molecular weight of the cooligomers were determined according to the data from NMR spectra. Signal assignments are listed in Table 4.

The M_n of the G^{3}OPG segments was determined according to the following equation:

$$M_n = (N_P + N_{Pe}) \cdot N_{Pe}^{-1} \cdot f \cdot M_P \tag{1}$$

M_P is the molecular weight of a single propylene glycol unit (58.1 g mol^{-1}) and *f* the number of functionalities of the star (*f* = 3). The relative number of the terminal propylene glycol units at the chain ends (N_{Pe}) and the propylene glycol units within the chain (N_P) were determined by ^{1}H-NMR signal integration. N_P is the sum of integrals of the signals of the methylene and methine protons of the internal propylene glycol units (CH$_2$-P and CH-P) divided by 3. N_{Pe} is the integral of the signal of the methylene protons of the terminal propylene glycol units (CH$_2$-P$_e$). The M_n of the P^{4}OLG precursors was determined according to the following equation:

$$M_n = (N_G \cdot M_G + N_L \cdot M_L) \cdot N_I^{-1} + M_I \tag{2}$$

M_L and M_G are the molecular weights of the monomers **3** and **4** respectively, and M_I of the initiator pentaerythrite **2**. The relative numbers of the monomer segments (N_G, N_L) and of the initiator (N_I) were determined by ^{1}H-NMR signal integration. N_G is the integral of the signal of the α-methylene protons of the glycolide units (CH$_2$-G) divided by 2. N_L is the integral of the signal of the methine protons of lactide units (CH-L) and N_I is integral of the signal of the methylene protons of initiator unit (CH$_2$-P^4) divided by 8. The M_n of the G^{3}OPG-OLG precursors was determined according to the above mentioned equation for the G^{3}OPG segments with M_I as the molecular mass of the respective initiating G^{3}OPG triol and N_I determined as the sum of integrals of the signals of the methylene and methine protons of the internal propylene glycol units (CH$_2$-P and

Table 3 Synthesis of polymer networks by crosslinking G³OPG or mixtures of G³OPG and P⁴OLG with TMDI

Sample ID[a]	P⁴OLG		G³OPG		TMDI	
	n (mmol)[b]	m (g)	n (mmol)[b]	m (g)	n (mmol)	V (µl)
N-G³OPG(1)	–	–	1.08	1.00	1.69	351.6
N-G³OPG(1;10)/P⁴OLG	0.08	0.87	0.11	0.10	0.34	71.4
N-G³OPG(1;20)/P⁴OLG	0.07	0.72	0.19	0.18	0.45	93.2
N-G³OPG(1;30)/P⁴OLG	0.21	2.15	0.98	0.91	1.97	409.4
N-G³OPG(1;50)/P⁴OLG	0.14	1.51	1.65	1.53	2.89	600.8
N-G³OPG(1;70)/P⁴OLG	0.08	0.86	2.37	2.20	3.90	809.4
N-G³OPG(3)	–	–	0.28	0.98	0.44	92.4
N-G³OPG(3;10)/P⁴OLG	0.09	0.91	0.03	0.10	0.23	47.3
N-G³OPG(3;20)/P⁴OLG	0.08	0.80	0.06	0.20	0.25	52.1
N-G³OPG(3;30)/P⁴OLG	0.07	0.73	0.09	0.31	0.29	59.6
N-G³OPG(3;50)/P⁴OLG	0.06	0.61	0.18	0.61	0.40	82.9
N-G³OPG(3;70)/P⁴OLG	0.08	0.86	0.65	2.26	1.20	248.8
N-G³OPG(6)	–	–	0.19	1.05	0.30	61.5
N-G³OPG(6;10)/P⁴OLG[c]	0.08	0.86	0.02	0.09	0.20	41.1
N-G³OPG(6;20)/P⁴OLG[c]	0.08	0.81	0.04	0.20	0.22	45.4
N-G³OPG(6;30)/P⁴OLG[c]	0.07	0.70	0.05	0.30	0.22	46.7
N-G³OPG(6;50)/P⁴OLG[c]	0.05	0.50	0.09	0.51	0.24	50.7

[a] N-G³OPG(x) are polymer networks from crosslinked G³OPG segments with the M_n ($x \times 1000$ g mol⁻¹) given in *parentheses*, N-G³OPG(x;y)/P⁴OLG are polymer networks obtained by crosslinking G³OPG segments with the M_n ($x \times 1000$ g mol⁻¹) and the mass fraction μ_{OPG} (y wt%) given in *parentheses*

[b] Calculation based on M_n derived from ¹H-NMR spectroscopic data

[c] Macroscopic phase separation lead to inhomogeneous materials

CH-P) divided by 3. The mass fraction of OPG (μ_{OPG}) of N-G³OPG/P⁴OLG networks was determined after treatment with trifluoroacetic acid comparing the signals of the fragments.

The GPC measurements were performed with a multidetector setup consisting of a LC1120 pump and 600 mm × 7.5 mm mixed-D column (Polymer Laboratories Ltd., Shropshire, UK), a combination of a differential viscosimetry/90° angle light-scattering detector (Viscotek GmbH, Weingarten, Germany), and a differential diffractometer (ERC Inc., Kawaguchi-City, Japan). Chloroform was used as eluent with a flow rate of 1.0 ml min⁻¹. Polystyrene standards (580–995600 g mol⁻¹) were applied for the universal calibration.

For the determination of the gel content G and the mass related degree of swelling S, a specified amount of polymer network film (m_r from 0.2 to 0.5 g) was swollen in a 50 ml mixture of chloroform and diethylether (volume ratio 1:1) for 24 h at room temperature. The mass of the swollen material m_q was weighted. After drying of the films to constant weight at 80°C in vacuum (1 mbar) the mass of these films was determined (m_d). The gel content is given by:

$$G = m_d/m_r \qquad (3)$$

The mass related degree of swelling was calculated according to the following equation:

$$S = \left(m_q/m_d\right) \qquad (4)$$

The differential scanning calorimetric measurements (DSC) were recorded on a Perkin-Elmer DSC 7 (Rodgau-Juegesheim, Germany). The temperature range was between −100 and 150°C depending on the thermal properties of the cooligomers and networks. The heating and cooling rates were 10°C min⁻¹. Thermal properties were determined from the second heating.

The tensile tests were performed on a ZWICK 1425 (Zwick GmbH & Co., Ulm, Germany) having a load sensor suitable up to 50 N and a thermo chamber. The deformation rate was 10 mm min⁻¹. The bone-shaped samples have dimensions of 10 mm × 3 mm (parallel area), a thickness of 0.1–0.3 mm and a free length of the clamped samples of 4–6 mm. They were annealed for 20 min at the operating temperature before each experiment.

Table 4 ^{1}H-NMR signal assignments

Samples	Chemical shift (ppm)	Multiplicity	Assigned protons[a]
G^{3}OPG triols[b]	0.90–1.30	m	CH$_3$-P/P$_e$
	3.18–3.23	m	CH-P$_e$
	3.27–3.45	m	CH-P
	3.45–3.76	m	CH$_2$-P
	3.87–3.98	m	CH$_2$-P$_e$
P^{4}OLG tetrols	1.40–1.70	m	CH$_3$-L/L$_e$
	4.05–4.25	s	CH$_2$-P^4
	4.23–4.32	m	CH$_2$-G$_e$
	4.32–4.44	m	CH-L$_e$
	4.50–4.90	m	CH$_2$-G
	5.00–5.30	m	CH-L
G^{3}OPG-*bl*-OLG triols[b]	1.00–1.15	m	CH$_3$-P
	1.15–1.28	m	CH$_3$-P$_e$
	1.35–1.60	m	CH$_3$-L/L$_e$
	3.22–3.40	m	CH-P/P$_e$
	3.40–3.76	m	CH$_2$-P/P$_e$
	4.09–4.28	m	CH$_2$-G$_e$
	4.28–4.43	m	CH-L$_e$
	4.45–4.90	m	CH$_2$-G
	4.95–5.30	m	CH-L
N-G^{3}OPG/P^{4}OLG[c]	0.82–1.07	d	CH$_3$-P$_f$
	1.08–1.60	d	CH$_3$-L$_f$
	3.10–3.65	d	CH-P$_f$/CH$_2$-P$_f$
	3.80–5.15	d	CH-L$_f$/CH$_2$-G$_f$

[a] Protons from pentaerythrite (P^4), propylene glycol (P), lactic acid (L) and glycolic acid (G), subscript e indicates a terminal unit at the end of the oligomer chain, a subscript f indicates a fragment

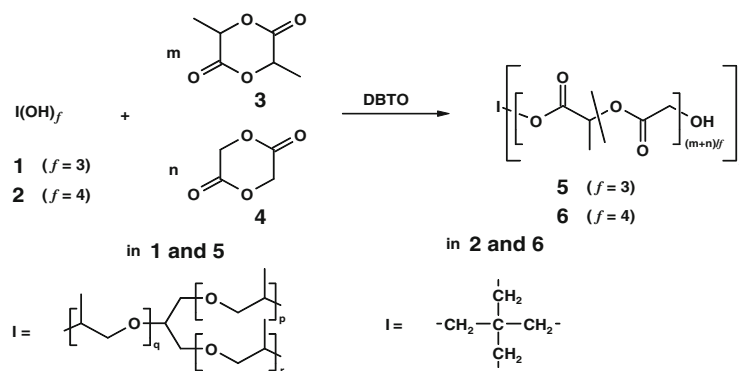[b] Signals of the initiator units were not detected

[c] Fragments of the networks after treatment with trifluoroacetic acid were investigated

[d] Complex of partially overlapping multiplets

3 Results and discussion

The two network architectures were expected to generate a tendency of microscopic phase segregation. Within the first set of polymer networks (N-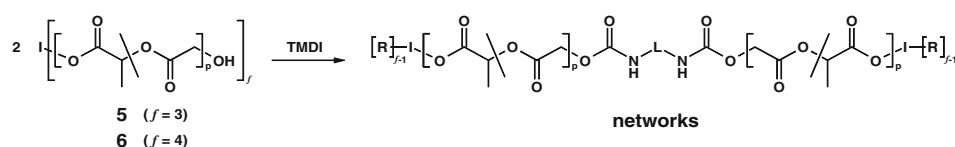G^{3}OPG-*bl*-OLG) three armed hydroxyl-telechels were crosslinked with diisocyanate forming diurethane bridges, which increase the block length of the OLG sequences. The second set of polymer networks contains a mixture of star-shaped G^{3}OPG and P^{4}OLG segments, which would separate phases macroscopically in a blend. Therefore, both sets of polymer networks are expected to show a more or less pronounced microscopic phase segregation.

The star-shaped co-oligoester segments that constitute the crosslink points within the polymer networks were synthesized by using either three-armed hydroxyl-telechelic G^{3}OPGs (**1**) or pentaerythrite (**2**) as initiators for ROP of the monomers *rac*-dilactide (**3**) and diglycolide (**4**, see Scheme 1). An undesirable blocky structure of the copolyesters due to differences in reactivity can be minimized by using tin-catalysts that also catalyze transesterification [21]. A mass ratio of the monomers of 15/85 was adjusted where the resulting copolymer has been shown to be amorphous and has been applied in medical applications previously [1, 19, 22].

G^{3}OPG(1), G^{3}OPG(3) and G^{3}OPG(6) (digit given in parentheses is M_n in 1000 g mol^{-1}) were used as macroinitiators in ROP for the synthesis of the G^{3}OPG-*bl*-OLG segments.

Polymer networks were synthesized by coupling of the precursors with an isomeric mixture of 1,6-diisocyanato-2,2,4-trimethylhexane and 1,6-diisocyanato-2,4,4-trimethylhexane (TMDI, see Scheme 2). The mixture of TMDI-isomers was chosen to further reduce the probability of the occurrence of crystalline domains within the networks. During the network synthesis the macromonomers have to be lowly viscous liquids in order to obtain a high extent of macroscopic homogeneity of the polymer network and to ensure a sufficient crosslink density.

Chemical composition of the polymer networks was controlled by variation of the mass fraction of the copolymers and the molecular weight of the G^{3}OPG segments. Homonetworks from G^{3}OPG triols were synthesized to investigate the influence of the OLG segments. For the G^{3}OPG-*bl*-OLG precursors the stoichiometric ratio of monomer/initiator was varied in order to obtain diblock

Scheme 1 Synthesis of star-shaped hydroxytelechelic precursors by ROP; I(OH)$_f$: initiator, *f*: number of functionalities of the initiator, *DBTO*: dibutyltin oxide

Scheme 2 Crosslinking of hydroxyltelechelic precursors; *I*: see Scheme 1, *L*: 2,2,4-trimethylhexylene or 2,4,4-trimethylhexylene segment, *R*: OLG segment

cooligomers with calculated molecular weights (M_{calc}) in the range from 2000 to 12000 g mol^{-1}. In the resulting polymer networks the length of the OLG segments (elongated over the diurethane bridge) as well as the density of crosslinks was thereby altered and dependencies for the resulting properties recorded. The P^{4}OLG tetrol (**6**) was synthesized with an initiator/monomer ratio that resulted in a calculated M_n value of 10000 g mol^{-1}. The segment length was chosen to be long enough to support phase segregation within the polymer network.

For all synthesized N-G^{3}OPG/P^{4}OLG polymer networks the content of G^{3}OPG (μ_{OPG}) in the reaction was varied between 10 and 70 wt% and the resulting μ_{OPG} within the polymer networks was determined after destruction of the covalent network structures with trifluoroacetic acid (TFA) and following ^{1}H-NMR spectroscopic analysis. *S* and *G* were also determined.

3.1 Characterization of the G^{3}OPG-*bl*-OLG triols

The M_n of the G^{3}OPG triols as well as of the obtained diblock-cooligomers was determined by ^{1}H-NMR spectroscopy and GPC analysis. These values of M_n and

the calculated values with respect to the initial weight of the starting materials (M_{calc}) are compared in Table 5.

The ratio of conversion (r_c) is given by means of the amount of transformed terminal hydroxyl groups relatively to the amount of hydroxyl groups in the starting material terminated by ^{1}H-NMR-spectroscopy. Hydroxyl-telechels with r_c above 90% are considered to mainly consist of the desired G^{3}OPG-*bl*-OLG. The application of G^{3}OPG(6) as initiator in the ROP for instance leads to hydroxyl-telechels with r_c lower than 90%, which implies a rather incomplete extent of defined terminal hydroxyl groups. Hence, these polymers were not used in the formation of the networks and not further characterized.

No melting or crystallization process was apparent for the G^{3}OPG-*bl*-OLG triols in DSC measurements that provides evidence for the oligomers to be completely amorphous. For the G^{3}OPG-*bl*-OLG triols synthesized from G^{3}OPG(1) and G^{3}OPG(3) only one glass transition was found. The T_g of the precursors decreased with decreasing M_n and consequentially increasing content of OPG (Fig. 2). The polymers represented a mixed phase system since for complete phase segregation the system was expected to

Table 5 Mass fraction μ_{OPG}, M_n according to NMR and GPC, ratio of conversion (r_c) and polydispersity (*D*) of G^{3}OPG-*bl*-OLG precursors and G^{3}OPG macroinitiators

Sample-ID[a]	μ_{OPG}—R[b] (wt%)	μ_{OPG}[c] (wt%)	M_{calc}[b] (g mol^{-1})	M_n (NMR)[c] (g mol^{-1})	M_n (GPC) (g mol^{-1})	*D* (GPC)	r_c[c] (%)
G^{3}OPG(1)	100	100	1000	930	1200	1.03	–
G^{3}OPG(1)-*bl*-OLG(2)	50	41	2000	2300	2700	1.09	95
G^{3}OPG(1)-*bl*-OLG(4)	25	22	4000	4200	6000	2.35	>99
G^{3}OPG(1)-*bl*-OLG(6)	17	14	6000	6500	6600	1.33	>99
G^{3}OPG(1)-*bl*-OLG(9)	11	10	9000	9000	8500	1.34	>99
G^{3}OPG(3)	100	100	3000	3400	3600	1.07	–
G^{3}OPG(3)-*bl*-OLG(4)	75	82	4000	4200	6100	1.01	95
G^{3}OPG(3)-*bl*-OLG(6)	50	54	6000	6500	11400	2.80	98
G^{3}OPG(3)-*bl*-OLG(9)	33	38	9000	9100	8700	1.41	92
G^{3}OPG(6)	100	100	6000	5600	7000	1.44	–
G^{3}OPG(6)-*bl*-OLG(9)	67	60	9000	9300	13400	1.65	86
G^{3}OPG(6)-*bl*-OLG(12)	50	48	12000	11700	7600	2.56	76

[a] G^{3}OPG(x) are commercially available three armed oligo(propylene glycol)s with the M_n ($x \times 1000$ g mol^{-1}, according to the manufacturer) given in *parentheses*, for G^{3}OPG(x)-*bl*-OLG(y) see Table 1 note a

[b] As calculated from the starting materials

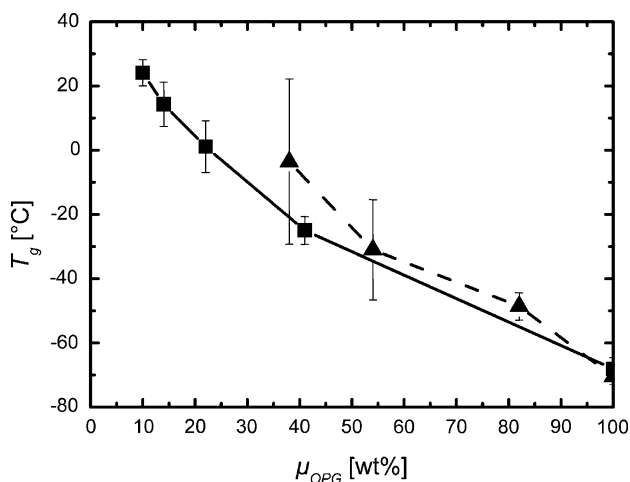[c] As determined by ^{1}H-NMR spectroscopy

Fig. 2 T_g (DSC, 2nd heat-up) of G^{3}OPG-*bl*-OLG triols as a function of the mass fraction of OPG (μ_{OPG} according to ^{1}H-NMR spectroscopy); the bars give the temperature interval of the glass transition; *filled square*—G^{3}OPG(1)-*bl*-OLG; *filled triangle-* -G^{3}OPG(3)-*bl*-OLG

Table 6 Gel content G and mass related degree of swelling S in chloroform of N-G^{3}OPG-*bl*-OLG networks

Sample ID[a]	G (%)	S (%)
N-G^{3}OPG(1)	97 ± 2	n.d.[b]
N-G^{3}OPG(1)-*bl*-OLG(2)	97 ± 2	350 ± 10
N-G^{3}OPG(1)-*bl*-OLG(4)	93 ± 4	870 ± 60
N-G^{3}OPG(1)-*bl*-OLG(6)	94 ± 1	960 ± 10
N-G^{3}OPG(1)-*bl*-OLG(9)	90 ± 1	1390 ± 130
N-G^{3}OPG(3)	98 ± 1	700 ± 10
N-G^{3}OPG(3)-*bl*-OLG(4)	94 ± 1	1330 ± 400
N-G^{3}OPG(3)-*bl*-OLG(6)	73 ± 1	3670 ± 10
N-G^{3}OPG(3)-*bl*-OLG(9)	58 ± 1	3650 ± 780

[a] N-G^{3}OPG(x) are polymer networks from crosslinked G^{3}OPG segments with the M_n ($x \times 1000$ g mol^{-1}) given in *parentheses*, N-G^{3}OPG(x)-*bl*-OLG(y) are polymer networks obtained by crosslinking G^{3}OPG(x)-*bl*-OLG(y) precursors, for G^{3}OPG(x)-*bl*-OLG(y) see Table 1 note a

[b] Not determined due to destruction of the networks during the swelling in chloroform

have two distinguishable glass transitions. The width of the range of the glass transition was considerably increased in case of the G^{3}OPG(3) containing polymers with an OPG-content of 38 or 54 wt%. This observation can be explained with the enhanced tendency of the system to form two segregated phases.

3.2 Characterization of the N-G^{3}OPG-*bl*-OLG polymer networks

The extent of phase segregation within the polymer network is influenced by the crosslink density and the chain segment length of the oligomer blocks. These parameters were changed by varying the mass ratio and molecular weight (length of chain segments) of the oligomeric precursors and the dependence of the formation of phase segregated networks with two distinguishable glass transition temperatures was analyzed.

Characterization of the polymer networks included determination of S and G obtained from swelling experiments in chloroform (Table 6). G of the G^{3}OPG(1) containing networks (between 90% and 97%) implied a nearly quantitative crosslinking whereas the G^{3}OPG(3) containing networks from hydroxyl-telechels with $M_n \geq 6000$ g mol^{-1} showed significant lower values of G. It was shown that S increased with increasing molecular weight of the polymer networks. The networks N-G^{3}OPG(3)-*bl*-OLG(6) and N-G^{3}OPG(3)-*bl*-OLG(9) showed significantly lower values of S than their G^{3}OPG(1) containing counterparts. This difference despite having OLG segments of similar length has been attributed to incomplete crosslinking.

In DSC measurements for each polymer network only one glass transition was found. It could be shown that T_g is a function of the OPG-content (Fig. 3). Higher values of T_g were detected for the polymer networks than for the underlying macrotriols. This trend was expected for a mixed T_g. As a result of an increased degree of crosslinking the OPG(1) containing network showed a higher T_g than the OPG(3) containing network. As already found for the hydroxyl-telechels the width of the range of the glass transition was considerably increased in case of the G^{3}OPG(3) containing networks with an OPG-content of 38 or 54 wt%. The effect was also comparable in quantity and
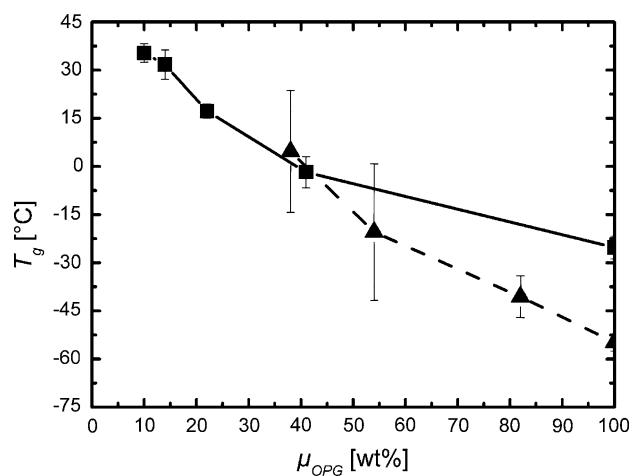

Fig. 3 T_g (from DSC, 2nd heat-up) of N-G^{3}OPG-*bl*-OLG networks as a function of the mass fraction of OPG within the precursors (μ_{OPG} according to ^{1}H-NMR spectroscopy); the bars give the temperature interval of T_g; *filled square*—N-G^{3}OPG(1)-*bl*-OLG; *filled triangle-* -N-G^{3}OPG(3)-*bl*-OLG

has been attributed to an incipient phase separation as a result of the less efficient mixing of the OPG and OLG chain segments. The mixed T_g increases with increasing chain length of the OLG segments in the direction of the T_g of the OLG precursors indicating a less effective phase mixing. However, it was shown that based on G³OPG(1) and G³OPG(3) no phase segregated polymer network was obtained and the G³OPG(6) containing precursors displayed an incomplete conversion of the terminal hydroxyl groups. Despite the extension of the OLG chains by linking two segments by diurethane junction units, no phase separation was achieved. Apparently the effect of the length extension of single OLG chain segments is not strong enough to lead to phase separation in the investigated polymer networks.

3.3 Characterization of the N-G³OPG/P⁴OLG polymer networks

In order to reduce the inhomogeneity of the material caused by macroscopic phase separation, the catalyst was added after the addition of the diisocyanate to the reaction mixture to start crosslinking at room temperature. For the synthesis of networks with at least 10 wt% of G³OPG(6) no homogeneous material could be obtained. These materials possess a high degree of macroscopic phase separation and were not further characterized. The high molecular mass of the G³OPG(6) segments strongly impedes the

mixing of the phases to an extent where macroscopic de-mixing was observed. For the polymer networks containing G³OPG(1) and G³OPG(3) segments the results of characterization are summarized in Table 7. The gel content of the networks slightly decreases with increasing content of G³OPG. S increases with the G³OPG content due to a lower density of crosslinking as shown by lower gel contents. The polymer networks show a macroscopic homogeneous appearance.

DSC measurements indicated that the networks were completely amorphous (see Fig. 4 for exemplary polymer networks). Neither melting range nor crystallization was observed. All polymer networks showed a T_g between 39 and 50°C that is related to a mainly OLG containing phase. This T_{g2} is between 2 and 8 K lower for the polymer networks with OPG(1) than for those with OPG(3) with the same content of OPG. That finding suggests that the content of OPG segments within the phase, which is represented by T_{g2} is higher in the polymer networks with the lower molecular weight of G³OPG segments.

If the content of OPG was higher than about 20 wt%, a second glass transition could be detected (T_{g1}). The T_g in G³OPG(1) containing polymer networks exceeds the one of the G³OPG(3) containing networks by 24–31 K. This attributes to the higher density of crosslinking and the higher content of OLG in the phase represented by this T_{g1}.

By applying the second network architecture, it was shown that the integration of star-shaped P⁴OLG tetrols

Table 7 Mass fraction of OPG in the reaction (μ_{OPG-R}) and mass fraction of OPG (μ_{OPG}), gel content (G), mass related degree of swelling (S) in chloroform, glass transition temperatures of N-G³OPG/P⁴OLG networks

Sample-ID[a]	μ_{OPG-R}[b] (wt%)	μ_{OPG}[c] (wt%)	G (wt%)	S (%)	T_{g1} (°C)	T_{g2} (°C)
N-P⁴OLG	0	0	98 ± 2	830 ± 80	–	53
N-G³OPG(1;10)/P⁴OLG	10	n.d.[d]	98 ± 8	680 ± 70	–	43
N-G³OPG(1;20)/P⁴OLG	20	10	91 ± 1	740 ± 20	–	42
N-G³OPG(1;30)/P⁴OLG	30	28	94 ± 1	720 ± 30	−35	43
N-G³OPG(1;50)/P⁴OLG	50	39	94 ± 7	830 ± 130	−26	39
N-G³OPG(1;70)/P⁴OLG	70	68	79 ± 3	1750 ± 70	−33	44
N-G³OPG(1)	100	n.d.[d]	97 ± 2	n.d.[d]	−25	–
N-G³OPG(3;10)/P⁴OLG	10	n.d.[d]	96 ± 8	810 ± 40	–	50
N-G³OPG(3;20)/P⁴OLG	20	16	92 ± 1	770 ± 40	−58	50
N-G³OPG(3;30)/P⁴OLG	30	28	92 ± 10	970 ± 20	−59	45
N-G³OPG(3;50)/P⁴OLG	50	57	90 ± 12	1340 ± 90	−57	47
N-G³OPG(3;70)/P⁴OLG	70	n.d.[d]	67 ± 1	2640 ± 10	−57	46
N-G³OPG(3)	100	n.d.[d]	98 ± 1	700 ± 10	−55	–

[a] N-P⁴OLG are networks from crosslinked P⁴OLG segments with M_n = 10000 g mol⁻¹, N-G³OPG(x) are polymer networks from crosslinked G³OPG segments with the M_n ($x \times 1000$ g mol⁻¹) given in *parentheses*, N-G³OPG(x;y)/P⁴OLG are polymer networks obtained by crosslinking G³OPG segments with the M_n ($x \times 1000$ g mol⁻¹) and the mass fraction μ_{OPG-R} (y wt%) given in *parentheses*

[b] As calculated from the starting materials

[c] As determined by ¹H-NMR-spectroscopy of the networks after treating with trifluoroacetic acid
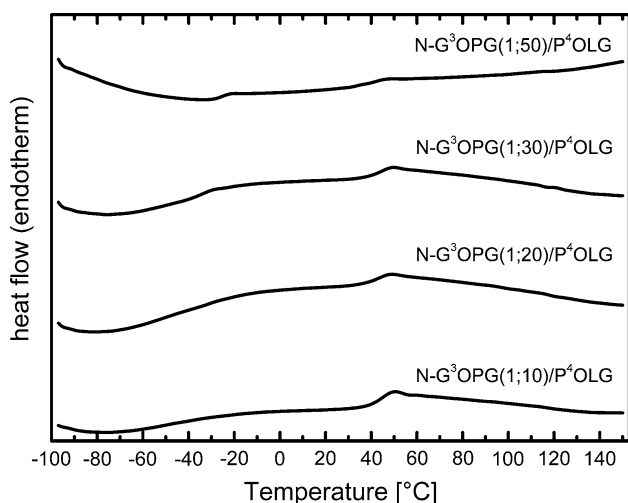
[d] Not determined

Fig. 4 DSC profiles of four exemplary N-G^{3}OPG(1)/P^{4}OLG polymer networks (2nd heat-up)
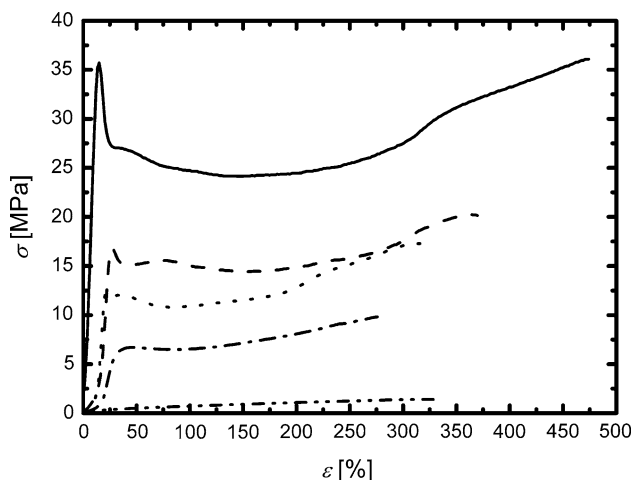

Fig. 5 Stress–strain-curves of N-G^{3}OPG(1)/P^{4}OLG networks at 25°C. — N-G^{3}OPG(1;10)/P^{4}OLG, - - N-G^{3}OPG(1;20)/P^{4}OLG, ···· N-G^{3}OPG(1;30)/P^{4}OLG, ⋯ N-G^{3}OPG(1;50)/P^{4}OLG, ⋯ N-G^{3}OPG(1;70)/P^{4}OLG; for identification of the networks see Table 7 note a

resulted in polymer networks with two segregated amorphous phases. The mass fraction of the OPG segments has influence on the detectability of T_{g1} being associated to the OPG phase.

The mechanical properties of the N-G^{3}OPG(1)/P^{4}OLG and the N-G^{3}OPG(3)/P^{4}OLG polymer networks were investigated by tensile tests at 25°C (see Fig. 5). In addition, the N-G^{3}OPG(1)/P^{4}OLG networks were investigated at 70°C in order to examine temperature dependencies and the mechanical properties above T_{g2}.

For an OPG content of less than 50 wt% a yield point could be observed. For higher OPG contents the stress–

Table 8 Mechanical properties of N-G^{3}OPG/P^{4}OLG networks at 25°C

Sample-ID[a]	E (MPa)	σ_b (MPa)	ε_b (%)
N-P^{4}OLG	340 ± 60	36.2 ± 5.9	250 ± 210
N-G^{3}OPG(1;10)/P^{4}OLG	250 ± 60	29.2 ± 8.8	375 ± 140
N-G^{3}OPG(1;20)/P^{4}OLG	120 ± 40	20.0 ± 2.0	525 ± 150
N-G^{3}OPG(1;30)/P^{4}OLG	150 ± 10	19.6 ± 1.7	450 ± 125
N-G^{3}OPG(1;50)/P^{4}OLG	43 ± 10	9.0 ± 0.5	335 ± 70
N-G^{3}OPG(1;70)/P^{4}OLG	2.0 ± 0.9	1.22 ± 0.2	325 ± 45
N-G^{3}OPG(1)	2.0 ± 0.3	0.96 ± 0.2	60 ± 15
N-G^{3}OPG(3;10)/P^{4}OLG	390 ± 20	32.1 ± 4.1	370 ± 10
N-G^{3}OPG(3;20)/P^{4}OLG	450 ± 20	26.3 ± 1.5	450 ± 15
N-G^{3}OPG(3;30)/P^{4}OLG	140 ± 20	17.2 ± 3.9	280 ± 195
N-G^{3}OPG(3;50)/P^{4}OLG	110 ± 20	13.1 ± 2.1	155 ± 30
N-G^{3}OPG(3;70)/P^{4}OLG	4.3 ± 0.9	2.98 ± 0.2	50 ± 15
N-G^{3}OPG(3)	0.9 ± 0.1	0.54 ± 0.1	85 ± 20

[a] For identification of the networks see Table 7 note a

strain curves resembled a typical trend for highly elastic materials. The determined values for the mechanical properties are listed in Table 8. The E-modulus (E) decreased with increasing OPG content. An exception is the N-G^{3}OPG(3,20)/P^{4}OLG with a slightly increased E compared to the polymer network containing 10 wt% G^{3}OPG(3). The increased E might be explained by a higher degree of crosslinking, which dominates the softening arising from a higher OPG content. This explanation is supported by a slightly lower S determined for that polymer network. The polymer networks containing G^{3}OPG(1) segments showed a considerably lower value for E than the networks containing G^{3}OPG(3) segments at low OPG contents. This observation can be attributed to the low T_g of the OLG-rich phase of these networks. The values for the tensile stress at break (σ_b) showed the same dependence. By changing the G^{3}OPG content of the N-G^{3}OPG/P^{4}OLG polymer networks the elasticity can be altered in a wide range with E values between 450 and 2 MPa at ambient temperature. For the G^{3}OPG(1) containing polymer networks the elongation at break (ε_b) remains above 300% with increasing OPG content. The ε_b of the polymer networks containing G^{3}OPG(3) segments decreased alongside the elasticity.

The stress–strain curves obtained from tensile stress tests with N-G^{3}OPG(1)/P^{4}OLG networks at 70°C showed a progression similar to elastomers. The determined values for E, σ_b and ε_b are shown in Table 9. A decrease of E and σ_b with increasing OPG content was observable. This finding is contrary to the expectation that a higher μ_{OLG} leads to a higher density of crosslinks. It can be explained by incomplete crosslinking where also the swelling experiments pointed to (Table 7).

Table 9 Mechanical properties of N-G^{3}OPG/P^{4}OLG networks at 70°C

Sample-ID[a]	E (MPa)	σ_b (MPa)	ε_b (%)
N-P^{4}OLG	1.86 ± 0.35	3.51 ± 0.21	470 ± 5
N-G^{3}OPG(1;10)/P^{4}OLG	2.21 ± 0.42	2.50 ± 0.67	275 ± 115
N-G^{3}OPG(1;20)/P^{4}OLG	2.04 ± 0.20	1.61 ± 0.23	170 ± 10
N-G^{3}OPG(1;30)/P^{4}OLG	1.67 ± 0.25	1.37 ± 0.05	165 ± 35
N-G^{3}OPG(1;50)/P^{4}OLG	1.53 ± 0.13	1.00 ± 0.14	100 ± 10
N-G^{3}OPG(1;70)/P^{4}OLG	0.21 ± 0.03	0.28 ± 0.06	225 ± 45

[a] For identification of the networks see Table 7 note a

4 Conclusion

Two concepts for the incorporation of a second amorphous phase in the synthesis of multiphase copolyesterurethane networks were investigated. In the first concept the cross-linking of the G^{3}OPG-*bl*-OLG prepolymers containing both segments lead to polymer networks with one glass transition representing a mixed phase. In these polymer networks phase segregation is structurally hindered. Phase segregated polymer networks were obtained applying the second concept where two different prepolymers representing the two different segments were crosslinked with diisocyanate. These N-G^{3}OPG/P^{4}OLG networks possess two distinct glass transitions with one T_g between −59 and −25°C and the second T_g between 39 and 53°C as well as good elastic properties with ε_b up to 500%. It has been shown that the mechanical properties could be adjusted by independently altering the two parameters content and molecular weight of the G^{3}OPG segments. With these polymers a promising new group of degradable biomaterials is available with properties being adjustable to meet the requirements of numerous medical applications.

References

1. Roby MS, Kennedy J Sutures. Biomaterial Science: An Introduction to Materials in Medicine. San Diego: Elsevier; 2004. p. 615.
2. Langer R, Vacanti JP. Tissue engineering. Science. 1993;260:920–6. doi:10.1126/science.8493529.
3. Li SM. Hydrolytic degradation characteristics of aliphatic polyesters derived from lactic and glycolic acids. J Biomed Mater Res. 1999;48:342–53. doi:10.1002/(SICI)1097-4636(1999)48:3<342::AID-JBM20>3.0.CO;2-7.
4. Jabbal-Gill I, Lin W, Kistner O, Davis SS, Illum L. Polymeric lamellar substrate particles for intranasal vaccination. Adv Drug Deliv Rev. 2001;51:97–111. doi:10.1016/S0169-409X(01)00173-9.
5. Witschi C, Doelker E. Influence of the microencapsulation method and peptide loading on poly(lactic acid) and poly(lactic-co-glycolic acid) degradation during in vitro testing. J Control Release. 1998;51:327–41. doi:10.1016/S0168-3659(97)00188-0.
6. Edelman ER, Nathan A, Katada M, Gates J, Karnovsky MJ. Perivascular graft heparin delivery using biodegradable polymer wraps. Biomaterials. 2000;21:2279–86. doi:10.1016/S0142-9612(00)00154-X.
7. Choi NY, Lendlein A. Degradable shape-memory polymer networks from oligo[(L-lactide)-ran-glycolide]dimethacrylates. Soft Matter. 2007;3:1–10. doi:10.1039/b702515g.
8. Bertmer M, Buda A, Blomenkamp-Höfges I, Kelch S, Lendlein A. Biodegradable shape-memory polymer networks: characterization with solid-state NMR. Macromolecules. 2005;38:3793–9. doi:10.1021/ma0501489.
9. Storey RF, Hickey TP. Degradable polyurethane networks based on D,L-lactide, glycolide, e-caprolactone and trimethylene carbonate homopolyester and copolyester triols. Polymer (Guildf). 1994;35:830–8. doi:10.1016/0032-3861(94)90882-6.
10. Kelch S, Choi NY, Wang Z, Lendlein A. Amorphous, elastic AB copolymer networks from acrylates and poly[(L-lactide)-ran-glycolide]dimethacrylates. Adv Eng Mater. 2008;10:494–502. doi:10.1002/adem.200700339.
11. Choi NY, Kelch S, Lendlein A. Synthesis, shape-memory functionality and hydrolytical degradation studies on polymer networks from poly(rac-lactide)b-poly(propylene oxide)-b-poly(rac-lactide) dimethacrylates. Adv Eng Mater. 2006;8:439–45. doi:10.1002/adem.200600020.
12. Smith SW, Freeman BD, Hall CK. Pressure-dependent photon correlation spectroscopic investigation of poly(propylene oxide) near the glass transition. Macromolecules. 1997;30:2052–7. doi:10.1021/ma960408+.
13. Alteheld A, Feng YK, Kelch S, Lendlein A. Biodegradable, amorphous copolyester-urethane networks having shape-memory properties. Angew Chem Int Ed. 2005;44:1188–92. doi:10.1002/anie.200461360.
14. Amsden B. Curable, biodegradable elastomers: emerging biomaterials for drug delivery and tissue engineering. Soft Matter. 2007;3:1335–48. doi:10.1039/b707472g.
15. Helminen A, Korhonen H, Seppälä JV. Biodegradable crosslinked polymers based on triethoxysilane terminated polylactide oligomers. Polymer (Guildf). 2001;42:3345–53. doi:10.1016/S0032-3861(00)00708-4.
16. Hild G. Model networks based on 'endlinking' processes: Synthesis, structure and properties. Prog Polym Sci. 1998;23:1019–149. doi:10.1016/S0079-6700(97)00055-5.
17. Palmgreen R, Karlsson S, Albertsson A-C. Synthesis of degradable crosslinked polymers based on 1, 5-dioxepan-2-one and crosslinker of bis-e-caprolactone type. J Polym Sci Part Polym Chem. 1997;35:1635–49. doi:10.1002/(SICI)1099-0518(19970715)35:9<1635::AID-POLA5>3.0.CO;2-Q.
18. Pitt CG, Hendren RW, Schindler A, Woodward SC. The enzymatic surface erosion of aliphatic polyesters. J Control Release. 1984;1:3–14. doi:10.1016/0168-3659(84)90016-6.
19. Valette L, Hsu CP. Polyurethane and unsaturated polyester hybrid networks: 2: influence of hard domains on mechanical properties. Polymer (Guildf). 1999;40:2059–70. doi:10.1016/S0032-3861(98)00428-5.
20. Younes HM, Bravo-Grimaldo E, Amsden BG. Synthesis, characterization and in vitro degradation of a biodegradable elastomer. Biomaterials. 2004;25:5261–9. doi:10.1016/j.biomaterials.2003.12.024.
21. Lendlein A, Neuenschwander P, Suter UW. Hydroxy-telechelic copolyesters with well defined sequence structure through ring-opening polymerization. Macromol Chem Phys. 2000;201:1067–76. doi:10.1002/1521-3935(20000701)201:11<1067::AID-MACP1067>3.0.CO;2-Y.
22. Yamaguchi K, Anderson JM. In vivo biocompatibility studies of medisorb® 65/35 D,L-lactide/glycolide copolymer microspheres. J Control Release. 1993;26:81–93. doi:10.1016/0168-3659(93)90169-6.